Statistical properties of high-lying chaotic eigenstates

1994 J. Phys. A: Math. Gen. 27 5509

(http://iopscience.iop.org/0305-4470/27/16/017)

J. Phys. A: Math. Gen. 27 (1994) 5509–5523. Printed in the UK

Statistical properties of high-lying chaotic eigenstates

Baowen Li† and Marko Robnik‡

Center for Applied Mathematics and Theoretical Physics, University of Maribor, Krekova 2, SLO-62000 Maribor, Slovenia

Received 7 April 1994

Abstract. We study the statistical properties of the high-lying chaotic eigenstates (200 000 and above) which are deep within the semiclassical regime. The system we are analysing is the billiard system inside the region defined by the quadratic (complex) conformal map of the unit disk as introduced by Robnik (1983). We are using Heller's method of plane-wave decomposition of the numerical eigenfunctions, and perform extensive statistical analysis with the following conclusions: (i) the local average probability density is in excellent agreement with the microcanonical assumption and all statistical properties are also in excellent agreement with the Gaussian random model; *(ii) the autocorrelation function is found to be strongly direction-*dependent and only after averaging over all directions agrees well with Berry's (1977) prediction; (iii) although the scars of unstable classical periodic orbits (in such an ergodic regime) are expected to exist, so far we have not found any (around the 200 000th state) other than a scar-like feature resembling the whispering-gallery modes.

1. Introduction

The field of quantum chaos is developing very quickly and there has been substantial progress in our understanding of generic properties of eigenstates in classically non-integrable and chaotic bound systems. In contrast to the theoretical description of the energy spectra (and of other quantal observables) where we now have a rather complete understanding of the spectral statistical universality classes and also of statistics in the transition region between integrability and ergodicity (i.e. going from Poisson to GOE/GUE), we are still far from a correspondingly complete knowledge of generic and statistical properties of the wavefunctions. For a few recent reviews see contributions in Giannoni *et al* (1991), Gutzwiller's book (1990), the papers in Casati *et al* (1993) and also the review on statistical properties of energy spectra by Robnik (1994).

In order to understand the wavefunctions, especially in the semiclassical limit, it is intuitively very appealing to use the so-called *principle of uniform semiclassical condensation* (PUSC) of the Wigner functions (of the eigenstates) which is implicit in Berry (1977a): as $\hbar \to 0$ we assume that the Wigner function of a given eigenstate uniformly (ergodically) condenses on the classical invariant object on which the classical motion is ergodic and which supports the underlying quantal state. Such an object can be, for example, an invariant torus, a chaotic region as a proper subset of the energy surface, or the entire energy surface if the system has ergodic dynamics there.

In classically integrable systems the eigenfunctions possess a lot of ordered structure *globally* and *locally*: applying PUSC, the average probability density in the configuration

† E-mail address: Baowen.Li@UNI-MB.SI
‡ E-mail address: Robnik@UNI-MB.SI

0305-4470/94/165509+15$19.50

space is seen to be determined by the projection of the corresponding quantized invariant torus onto the configuration space, which implies the global order. Moreover, the local structure is implied by the fact that the wavefunction in the semiclassical limit is locally a superposition of a finite number of plane waves (with the same wavenumber as determined by the classical momentum).

In the opposite extreme of a classically ergodic system, PUSC predicts that the average probability density is determined by the microcanonical Wigner function. Its local structure is spanned by the superposition of infinitely many plane waves with random phases and equal wavenumber. The random phases might be justified by the classical ergodicity and this assumption, originally due to Berry (1977b), is a good starting approximation which immediately predicts locally the Gaussian randomness for the probability amplitude distribution. Berry (1977b) has also calculated the autocorrelation function of semiclassical chaotic (ergodic) wavefunctions, which we will discuss later on in detail. One major surprise in this research was Heller's discovery (1984) of scars of unstable classical periodic orbits in classically ergodic systems. The scar phenomenon is, of course, a consequence of subtle correlations in the quantal phases. This has been analysed and discussed by Bogomolny (1988) and Berry (1989) in the context of the Gutzwiller periodic orbit theory. The insufficiency of the single-periodic-orbit theory of scars has been discussed by Prosen and Robnik (1993a) in a study of the transition region between integrability and chaos.

In the generic case of a KAM-like system with mixed classical dynamics, the application of PUSC is again very useful and has great predictive power. Here the states can be classified as either regular (they 'live' on a quantized invariant torus) or irregular (they 'live' on a chaotic invariant region), quite in agreement with Percival's (1973) speculative prediction, which has recently been carefully re-analysed by Prosen and Robnik (1994a). In this case PUSC implies asymptotic ($\hbar \to 0$) statistical independence of level series (subsequences) associated with different regular and irregular components. This picture has been used by Berry and Robnik (1984) to deduce the resulting energy level statistics in such generic Hamilton systems with mixed classical dynamics, especially the level spacing distribution. In a recent work Prosen and Robnik (1994b) have confirmed numerically the applicability of the Berry–Robnik theory and also explained the Brody-like behaviour (as discovered and described in Prosen and Robnik (1993b)) before reaching the far semiclassical limit.

2. The definition of the billiard system and the numerical technique

In the present paper we study the chaotic wavefunctions in the two-dimensional billiard system whose domain $\mathcal{B}$ (in the w-plane) is defined by the complex quadratic conformal map of the unit disk (in the z-plane), namely

$$\mathcal{B}_\lambda = \{w | w = z + \lambda z^2, |z| \leqslant 1\} \tag{1}$$

as introduced by Robnik (1983, 1984) and further studied by Prosen and Robnik (1993b) (see also Hayli *et al* (1987) and Bruus and Stone (1994), Stone and Bruus (1993, 1994)). Following most people in the field we shall refer to it as the Robnik billiard. As the shape parameter λ changes from 0 to $\frac{1}{2}$ this system goes from the integrable case of the circular billiard continuously through a KAM-like regime to an almost ergodic regime at large λ. At $\lambda \leqslant \frac{1}{4}$ the boundary is convex and therefore the Lazutkin-like caustics and invariant tori (of boundary glancing orbits) exist. At $\lambda \geqslant \frac{1}{4}$ the billiard was speculated (based on numerical evidence in Robnik (1983)) to become ergodic, which has been disproved by Hayli *et al* (1987): close to $\lambda \geqslant \frac{1}{4}$ there are still some stable periodic orbits surrounded by very tiny stability islands. On the other hand, for $\lambda = \frac{1}{2}$ (the cardiod billiard) the ergodicity and

mixing have been proved rigorously by Markarian (1993). Nevertheless, at large values of λ, say $\lambda = 0.375$ (which we study exclusively in the present paper), the numerical evidence does not exclude the possibility of ergodicity: if there are some tiny regions of stability, then they must be so small that they cannot be detected at large scales.

We want to calculate and analyse the high-lying states far within the semiclassical limit, as high as the 100 000th eigenfunction (of even parity which is about the 200 000th when counting all states) and above, in the regime where the classical dynamics is almost completely ergodic (within the numerical resolution of the Poincaré surface of section). As mentioned above, the latter condition is satisfied at $\lambda = 0.375$. However, in order to reach the said high-lying eigenstates using the available supercomputer facilities we had to abandon the conformal mapping diagonalization technique developed by Robnik (1984) and further employed by Prosen and Robnik (1993b). Instead we have implemented Heller's method of plane-wave decomposition of the wavefunctions (for example, see Heller 1991). Heller's method enables one to go very high in the semiclassical limit (high energies) where we can then calculate a few consecutive levels, whereas the diagonalization method (with the conformal mapping technique) has the advantage of yielding many levels from the ground state upwards. So, if one is interested in significant statistical analysis the latter method is superior, whilst when studying the individual high-lying eigenstates the former method is the better one.

Let us spend just a few words on the technical aspects of this difficult task, since to the best of our knowledge many crucial ingredients have not been discussed in the literature so far. To solve the Schrödinger equation with Dirichlet boundary conditions

$$\Delta\Psi + E\Psi = 0 \qquad \Psi = 0 \quad \text{at the boundary} \tag{2}$$

we use the superposition of plane waves with the wavevectors of the same magnitude k but with different directions. The wavefunction we used for the even parity is

$$\Psi(u, v) = \sum_{j=1}^{N} a_j \cos(k_{ju}u + \phi_j)\cos(k_{jv}v) \tag{3}$$

where $k_{ju} = k\cos(\theta_j)$, $k_{jv} = k\sin(\theta_j)$, $k^2 = E$ the eigenenergy, N the number of plane waves and ϕ_j are *random phases* drawn from the interval $[0, 2\pi)$, assuming uniform distribution, and $\theta_j = 2j\pi/N$ (i.e. the direction angles of the wavevectors are chosen equidistantly). The ansatz (3) solves the Schrödinger equation (2) in the *interior* of the billiard region, so that we have only to satisfy the Dirichlet boundary condition. Taking the random phases, as we discovered, is equivalent to spreading the origins of plane waves all over the billiard region, and at the same time this results in reducing the CPU time by almost a factor of ten. For a given k we put the wavefunction equal to zero at a finite number M of boundary points (primary nodes) and equal to 1 at an arbitrarily chosen interior point. Of course, $M \geqslant N$. This gives an inhomogeneous set of equations which can be solved by matrix inversion. Usually the matrix is very singular, thus the *singular value decomposition* (SVD) method has been invoked (Press *et al* 1986). After obtaining the coefficients a_j we calculate the wavefunctions at other boundary points (secondary nodes). The sum of the squares of the wavefunction at all the secondary nodes (Heller called this sum 'tension') would ideally be zero if k^2 is an eigenvalue. In practice, it is a positive number. Therefore the eigenvalue problem now is to find the minimum of the 'tension'. In our numerical procedure we have looked for the zeros of the first derivative of the tension; namely the derivative is available analytically/explicitly from (3) once the amplitudes a_j have been found. In fact, since the SVD method is based on finding the least-squares solution of the linear equations, we can choose M larger than N without running into the over-determination

problem. Indeed, this has been done with a typical choice $M = \frac{5}{3}N$. It must be pointed out that the wavefunctions obtained in this way are not (yet) normalized, due to the arbitrary choice of the interior point where the value of the wavefunction has been arbitrarily set equal to unity. We therefore explicitly normalize these wavefunctions before embarking to the analysis of their statistical properties.

The accuracy of this method, of course, depends on the number of plane waves (N) and on the number of the primary nodes (M), and we have a considerable freedom in choosing N and $M \geqslant N$. In order to reach a sufficient accuracy experience shows that we should take at least $N = 3\mathcal{L}/\lambda_{\text{de Broglie}}$, and $M = \frac{5}{3}N$, where $\mathcal{L}$ is the perimeter of the billiard and $\lambda_{\text{de Broglie}}$ is the de Broglie wavelength $= 2\pi/k$. With this choice we reach the double precision accuracy (sixteen digits) for all levels of integrable systems like the rectangular billiard (where the eigenenergies can be given trivially analytically) and the circular billiard, but also for the billiard $\mathcal{B}_\lambda$ for $\lambda \leqslant 0.2$. Also, the same choice enabled us to calculate the 100 000th even-parity eigenstate and a few nearby eigenstates for our billiard at $\lambda = 0.375$ within an accuracy of 1% of the mean level spacing (seven valid digits). These accuracy checks were based on very careful self-consistent checks of the method and also on comparison of the eigenvalues with those obtained by using Robnik's diagonalization method.

The advantage of this method is that, on one hand, it is very flexible for calculating the eigenvalues, and on the other hand, it is self-checkable: the accuracy and the reliability can be checked by changing the interior point and by changing N as well as M. The drawback of the method is that, with an unlucky choice of the interior point and an unlucky energy step size, some eigenstates may be—and typically are!—missed, so that the calculation must be repeated by using different interior points to finally collect all the levels. The Weyl formula (with perimeter and curvature corrections) can be used to detect the missing of levels (cf Bohigas 1991). A similar numerical experience has been reported in Frisk (1990).

3. The wavefunctions and the probability amplitude distribution

All the wavefunctions that we have calculated and discussed here are the even-parity eigenstates of the billiard $\mathcal{B}_\lambda$ at $\lambda = 0.375$. In figure 1 we plot the even-parity eigenfunction of energy $E = 625\,084.5$, which is about the 100 010th eigenstate of even parity, as estimated by using the Weyl formula (with perimeter and curvature corrections)

$$N_{\text{even}}(E) = \frac{1+2\lambda^2}{8}E - \frac{(1+2\lambda)E(\sqrt{8\lambda}/(1+2\lambda)) - 1}{2\pi}\sqrt{E} - \frac{1}{24} \tag{4}$$

where $E(x)$ is the complete elliptic integral of second kind (cf Prosen and Robnik 1993b).

This is a good example of a chaotic quantum eigenstate, which exhibits the characteristic filamentary structure as noticed already by Heller *et al* (1987, 1991), which is a consequence of the fact that in the ansatz (3) all plane waves (with random phases) have the same magnitude k of the wavevector. Also, as judged by the naked eye, the average probability density is constant only if the local averaging region is sufficiently large in units of de Broglie wavelength: probably we need a typical size of at least several ten wavelengths. The local and global average value $\langle\Psi^2\rangle$ is theoretically expected to be equal to $1/\mathcal{A}$, where $\mathcal{A} = \pi(1+2\lambda^2)$ is the area of $\mathcal{B}_\lambda$. This is a direct consequence of the microcanonically uniform Wigner function for this eigenstate (Berry 1977, Voros 1979, Shnirelman 1979; see also Berry 1983), which in turn is a consequence of PUSC as explained and discussed in the introduction. Indeed, the theoretical value of $\langle\Psi^2\rangle$ is 0.248 44, whereas the numerical evaluation yields 0.248 32 (after averaging over 1 145 294 grid points distributed uniformly

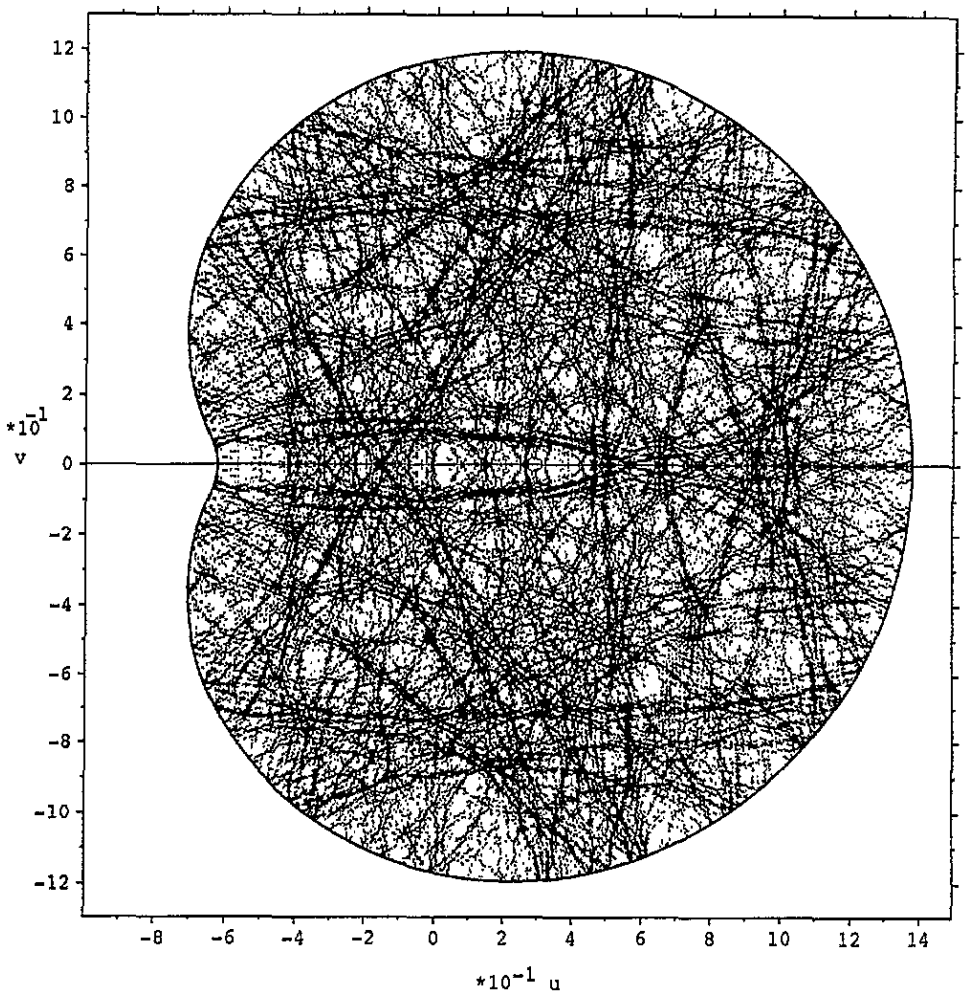

Figure 1. The probability density plot for the even-parity eigenstate with $E = 625\,084.5$, for $\lambda = 0.375$, and with the estimated sequential number using the Weyl formula (4) equal to 100 010. The contours are plotted at ten equally spaced steps between zero and the maximum value. In this geometry the unit length is 126 de Broglie wavelengths.

inside the interior of the billiard region), which can be considered as an excellent agreement. In table 1 we compare the theoretical values and the numerical estimates for a number of eigenstates to show that quite generally this agreement is very good. There we give the numerical estimate for all the lowest four moments of the Ψ-distribution, namely the average $m_1 = \langle\Psi\rangle$, the variance $m_2 = \langle(\Psi - m_1)^2\rangle$, the skewness $m_3 = \langle(\Psi - m_1)^3\rangle/m_2^{3/2}$ and the kurtosis $m_4 = \langle(\Psi - m_1)^4\rangle/m_2^2 - 3$. These experimental values are compared with the theoretical values of the Gaussian random model (see the introduction) which predicts

$$P(\Psi) = \frac{1}{\sqrt{2\pi}\sigma} \exp\left\{-\frac{\Psi^2}{2\sigma^2}\right\} \tag{5}$$

where again, according to PUSC, $\sigma^2 = 1/\mathcal{A} = 1/(\pi(1 + 2\lambda^2))$, and ideally it should be equal to m_2. In figures 2(a) and (b) we plot the numerical histogram for $P(\Psi)$

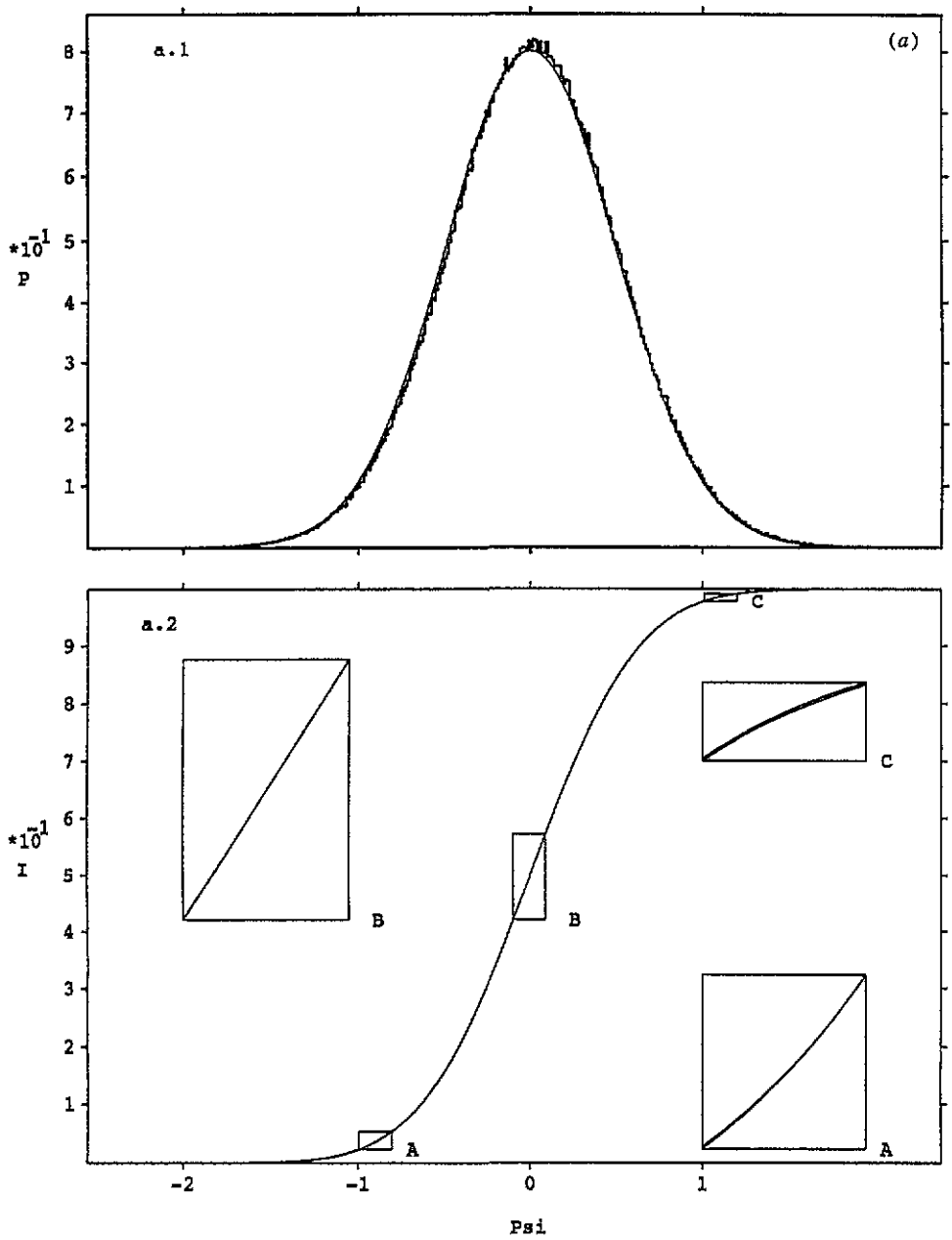

Figure 2. The probability distribution function and cumulative distribution function of eigenstates (*a*) $E = 625\,084.5$ (approximately 100 010th even-parity state), and (*b*) $E = 625\,118.4$ (approximately 100 015th even-parity state) in comparison with the Gaussian random model (5). In the upper diagrams we show the histograms compared with the theoretical curve (5), and in the lower diagrams we show the cumulative amplitude distribution function $I(\Psi)$. Three small boxed regions are displayed in the corresponding magnified windows. Here the difference between the theoretical and the numerical curves is hardly visible since the agreement is so good.

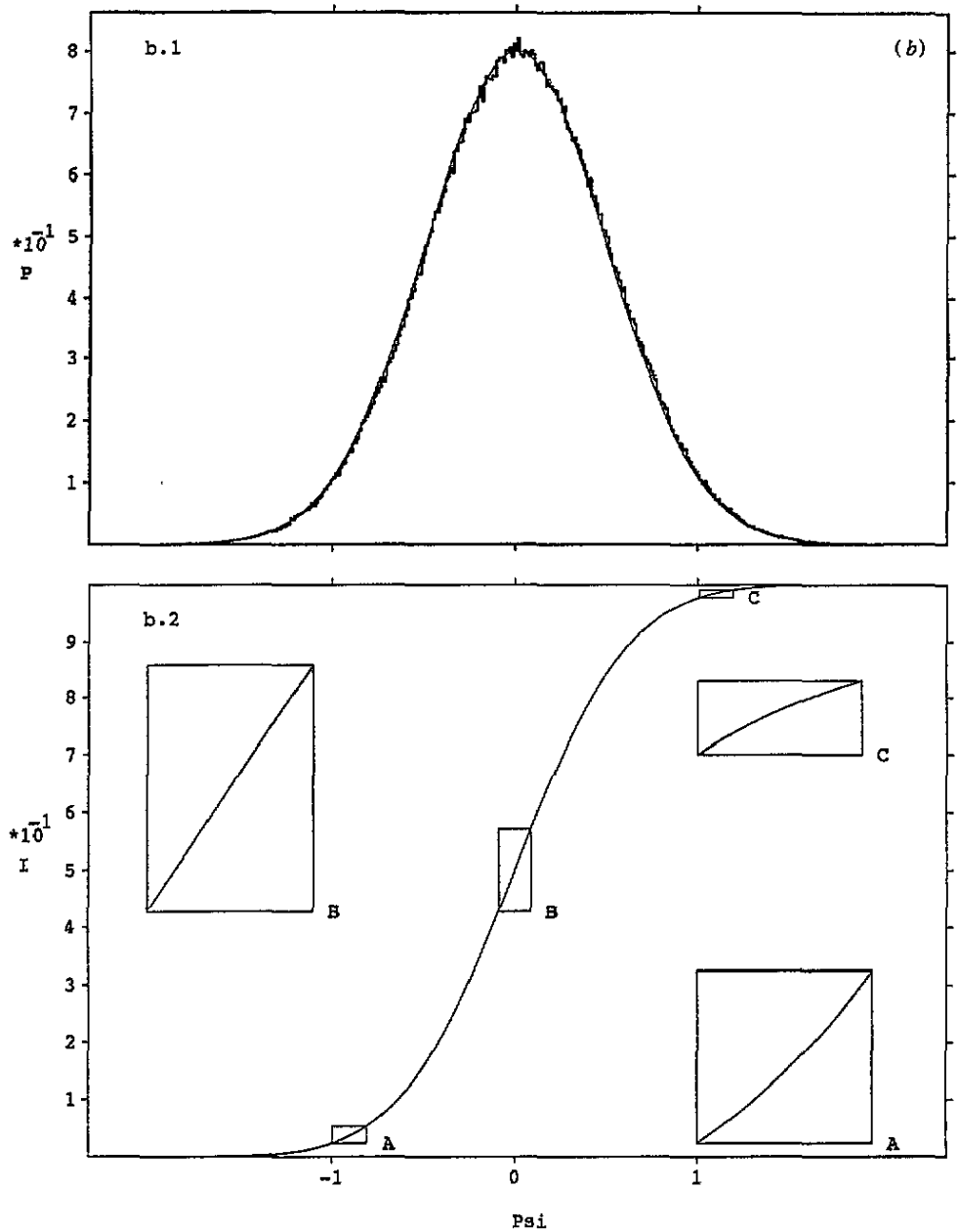

Figure 2. Continued.

(merely for illustrative purposes), and—more importantly—the cumulative distribution $I(\Psi) = \int_{-\infty}^{\Psi} P(x)\,dx$ which is compared with the theoretical model (5). The agreement is seen to be excellent, even in figure 2(*b*) where, as we shall see and discuss in section 5, in the probability density plot of the underlying wavefunction a scar-like feature is observed.

In addition, we have estimated the significance levels of the cumulative distribution $I(\Psi)$ according to the Kolmogorov–Smirnov test (Press *et al* 1986 p 472) with respect to

Table 1. The average, variance, skewness and kurtosis of a few eigenstates nearby the 100 000th eigenstate of even parity in comparison with theoretical values. $N_{ev}(E)$ is given by the Weyl formula (4). The significance levels of the Kolmogorov–Smirnov test for all eigenstates listed in this table are exactly one within 5 digits.

E	$N_{ev}(E)$	Average	Variance	Skewness	Kurtosis
625 040.6	100 003	0.000 02	0.248 28	−0.002 11	0.116 07
625 058.4	100 006	0.000 01	0.248 36	0.004 41	0.065 76
625 084.5	100 010	0.000 01	0.248 32	−0.001 60	0.068 09
625 099.5	100 012	−0.000 01	0.248 34	−0.001 79	0.036 38
625 118.4	100 015	0.000 01	0.248 38	0.004 60	−0.014 15
625 161.9	100 022	0.000 03	0.248 37	0.003 47	0.024 24
625 172.8	100 024	0.000 07	0.248 39	−0.002 48	0.048 36
625 182.1	100 025	0.000 00	0.248 54	−0.001 35	0.036 24
Gaussian		0.0	0.248 44	0.0	0.0

the Gaussian distribution for all eigenstates listed in table 1. It is found to be exactly 1 within five digits. This shows again that indeed our results agree excellently with the theoretical prediction.

A similar study of chaotic eigenfunctions has been published in Chirikov *et al* (1989), where even the differences between the numerical values and the Gaussian random model due to the finite dimensionality of the system have been seen.

Our results are comparable to the findings of Aurich and Steiner (1993) who studied the chaotic wavefunctions of the quantum system whose classical counterpart is the geodesic motion on a compact surface of constant negative curvature, although with our numerical wavefunctions we are considerably farther into the semiclassical limit. So far we have not found any examples of scars in these high-lying states around the 100 000th (however, see section 5). The conclusion is that scars are difficult to find since they 'live' on smaller and smaller support as $\hbar \to 0$, or $E \to \infty$, and consequently asymptotically no longer influence the $P(\Psi)$ distribution, as further explained in section 5.

4. The autocorrelation function of the wavefunctions

The mean statistical properties of chaotic wavefunctions have been discussed, analysed and described in the previous section. However, the question of space correlations of a wavefunction is far from trivial. The correlations exist on different scales and their strength can vary substantially. For example, in figure 1 we clearly see that there is some kind of clustering on the scale of a few tens of de Broglie wavelengths: there are regions of this size with enhanced probability density, and there are also regions of this size with notably depleted probability density (holes). Not every state is like that and in figure 3 we show another chaotic even-parity eigenstate with energy $E = 625\,118.4$, approximate number $N_{ev} = 100\,015$, again for $\lambda = 0.375$. Here the above-mentioned clustering is much less pronounced and this property is well captured in the autocorrelation function of the eigenstates, as we shall see in a moment.

The definition of the autocorrelation function of the probability amplitude of a given eigenstate is (Berry 1977b, 1983)

$$C(\boldsymbol{X}; q) = \langle \Psi(q + \boldsymbol{X}/2)\Psi^*(q - \boldsymbol{X}/2)\rangle / \langle |\Psi(q)|^2 \rangle \tag{6}$$

where the local average denoted by $\langle \cdots \rangle$ is taken over a sufficiently large region around

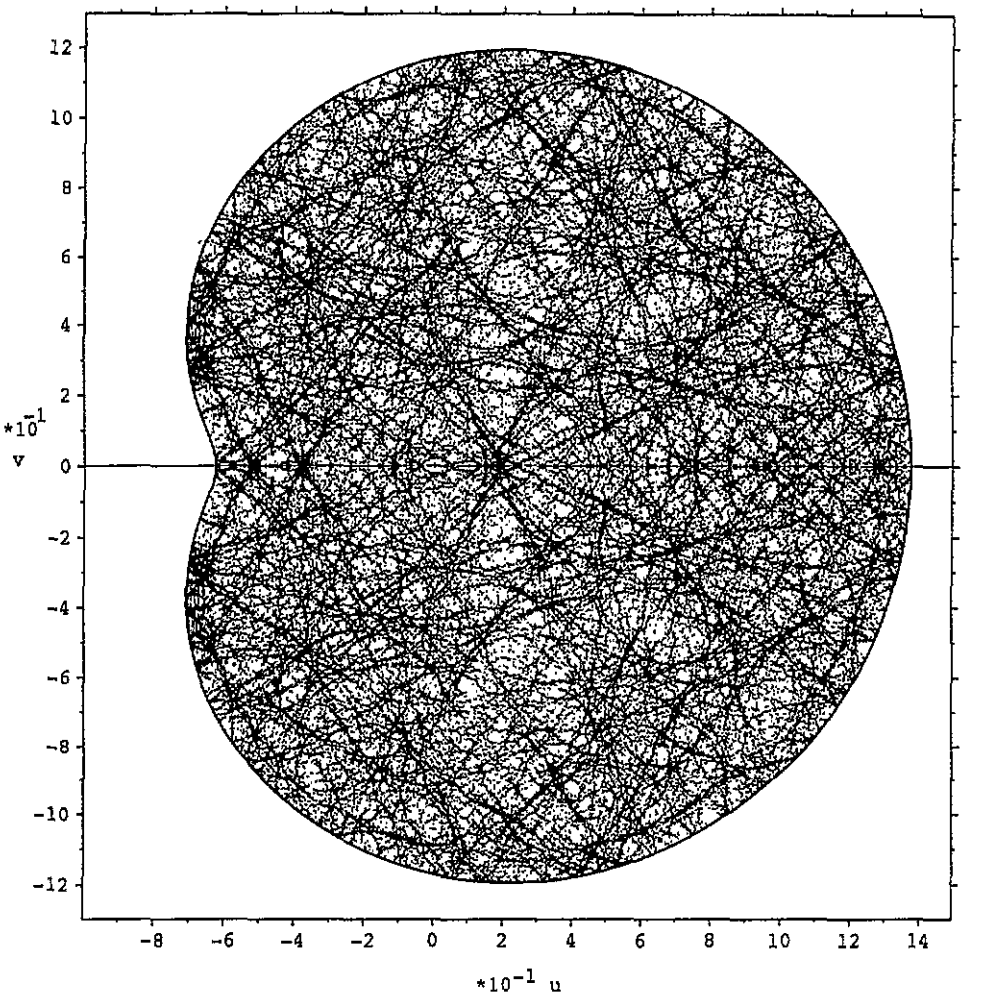

Figure 3. The probability density plot for the even-parity eigenstate with $E = 625\,118.4$, for $\lambda = 0.375$, and the estimated sequential number using the Weyl formula (4) equal to 100 015. The contours are plotted at ten equally spaced steps between zero and the maximum value. In this geometry the unit length is 126 de Broglie wavelengths.

q whose size is typically many de Broglie wavelengths but still small compared with the geometrical size. In our case the wavefunction is of course real, i.e. $\Psi^* = \Psi$. It should be noted that the denominator in (6) is actually the Fourier transform of the Wigner function $W(q, p)$,

$$W(q,p) = \frac{1}{(2\pi)^2} \int \mathrm{d}^2 X \exp(-\mathrm{i}p \cdot X)\Psi(q - X/2)\Psi(q + X/2) \tag{7}$$

where we have specialized to our real Ψ case, and also two degrees of freedom and $\hbar = 1$. Now using the PUSC for a chaotic state following Berry (1977b) we assume that the Wigner function of such a classically ergodic state is microcanonical, i.e.

$$W(q,p) = \frac{\delta(E - H(q,p))}{\int \mathrm{d}^2 q\, \mathrm{d}^2 p\, \delta(E - H(q,p))}. \tag{8}$$

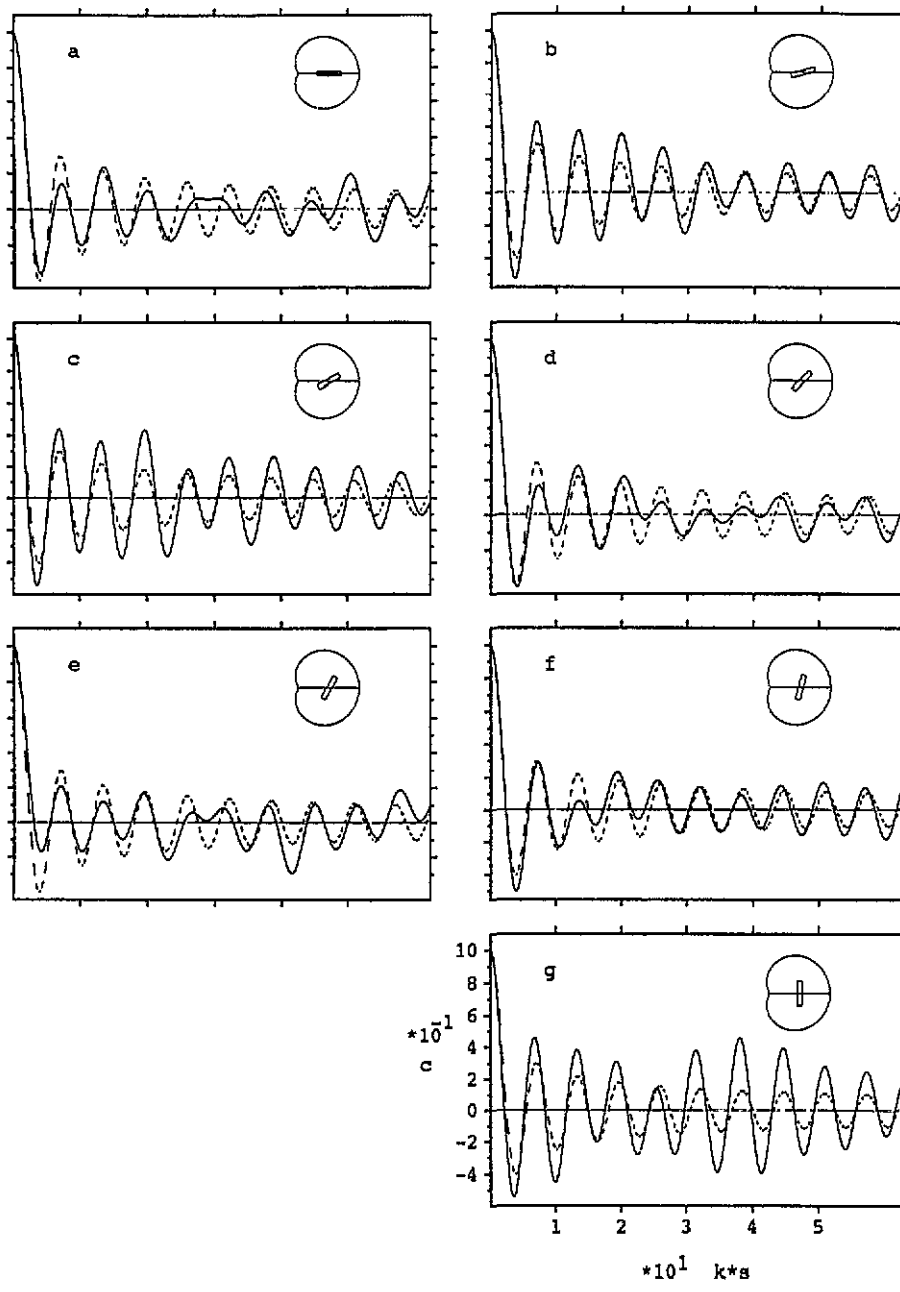

Figure 4. The autocorrelation function $C(X, q)$ of the eigenstate in figure 1. $C(X, q)$ is plotted against ks for seven different angles of X with respect to the abscissa; here $s = |X|$. The angle and the averaging strip are indicated in the upper right-hand corner of the figure. From (a) to (g) the angle goes from 0 to $\pi/2$ with an increment of $\pi/12$. The dashed curve is the theoretical prediction (9), namely $J_0(ks)$, whilst the full curve denotes the numerical result. The local average has been taken on a strip of 20×100 de Broglie wavelengths. For a fixed ks about 150 000 grid points inside the strip have been used to calculate C. The reference point q is fixed at (0.4, 0.0) which is probably sufficiently far away from the billiard boundary.

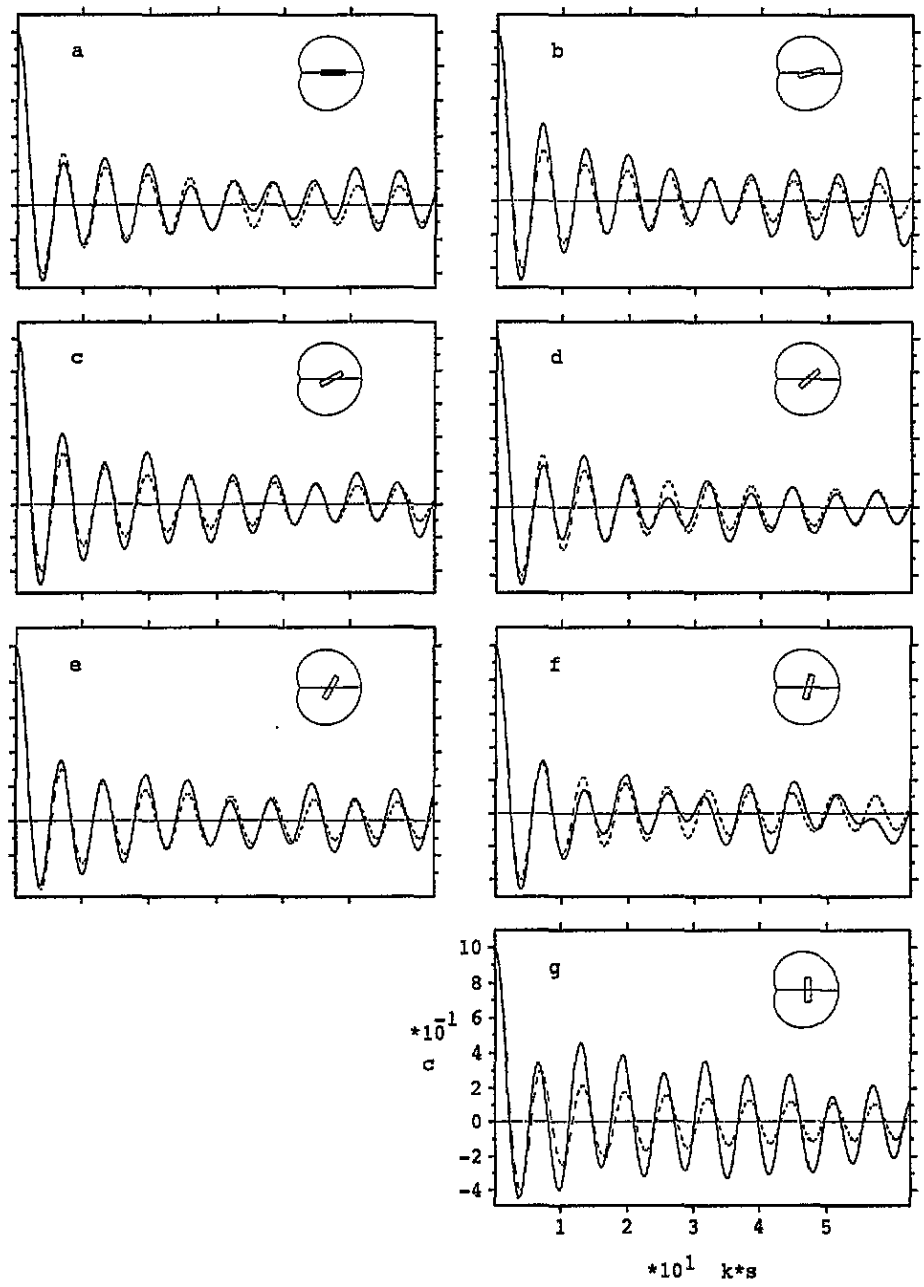

Figure 5. The same as figure 4, but for the eigenstate of figure 3.

Thus substituting (8) into the inversion of (7) and then into (6) we immediately obtain the special case of Berry's (1977b) result, namely

$$C(\boldsymbol{X}; q) = J_0(ks) \tag{9}$$

where J_0 is the Bessel function of zero order, k^2 is the eigenenergy and s is the length of $\boldsymbol{X}$. So the autocorrelation function is isotropic, and we are going to check numerically the

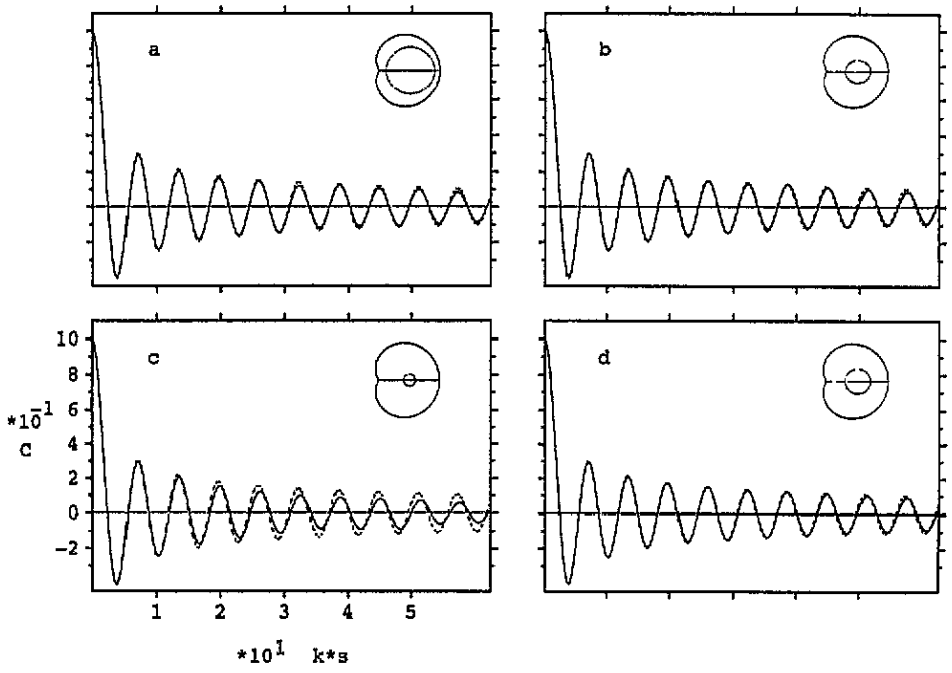

Figure 6. The autocorrelation function after averaging over many directions X of the eigenstate in figure 1. $C(X, q)$ is plotted against ks for three different averaging disks and different number of directions, where $s = |X|$. The averaging disk in (a), (b), (c) and (d) has a diameter of 200, 100, 50 and 100 de Broglie wavelengths, respectively. In (a), (b) and (c) the number of directions is 200, whilst in (d) it is 400.

validity of this theoretical prediction.

First we would like to check the isotropy of the autocorrelation function. To this end we have evaluated (6) by taking the local average on a small strip of 20×100 wavelengths situated at the centre of the billiard as far as possible from the boundaries. The results for the wavefunctions of figure 1 and figure 3 are shown in figures 4 and 5, correspondingly. Because of the inversion symmetry of the autocorrelation function with respect to X and the reflection symmetry of the wavefunctions Ψ with respect to v we can restrict ourselves to the angles within the interval $[0, \pi/2]$, and we have chosen the values between 0 and $\pi/2$ in equal steps of $\pi/12$, as indicated in the upper right-hand corner of the figures. The autocorrelation function is obviously strongly direction-dependent (please notice that the statistical noise is practically zero) and in the case of the more uniformly chaotic wavefunction of figure 3 agrees better with the theoretical prediction (9) than for the less chaotic eigenstate of figure 1. We believe that the semiclassical periodic orbit theory (see, for example, Casati *et al* 1993, Tél and Ott 1993 and references therein) could explain the deviations from the isotropy. Our results agree qualitatively with Aurich and Steiner (1993) although we are considerably higher in the semiclassical limit (by a factor of 10 or so), and also with somewhat old results in McDonald and Kaufman (1988), Shapiro and Goelman (1984), Shapiro *et al* (1988).

It is interesting that after averaging over many directions we get a considerable agreement with (9). This is shown in figures 6(a)–(d) where we vary the size of the averaging disk and also the number of the directions over which the average is taken. These

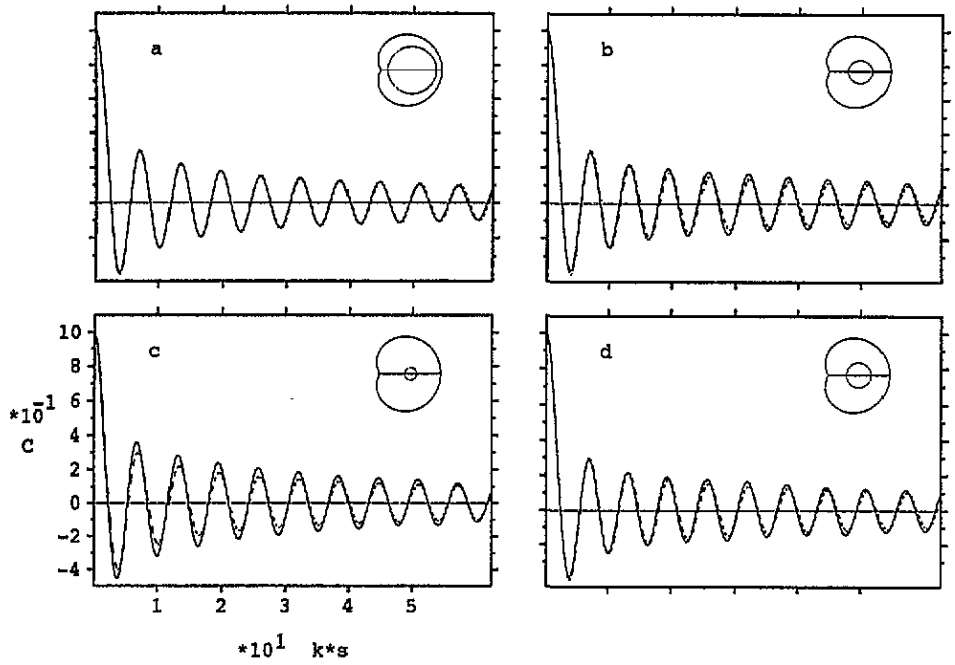

Figure 7. The same as in figure 6, but for the eigenstate in figure 3.

plots are for the eigenfunction shown in figure 1. Both effects are clearly visible, namely the increasingly better agreement with (9) as we increase the radius of the averaging disk and/or as we increase the number of directions. The same aspects are shown in figures 7(*a*)–(*d*) for the more uniformly chaotic state of figure 3. By comparing the figures 6(*a*) and 7(*a*) we see that in the latter plot the agreement with theory is better.

5. Scar-like features in wavefunctions

As we know since Heller's (1984) discovery of scars (of unstable classical periodic orbits) in chaotic quantum eigenfunctions of classically ergodic systems, we do expect such scars to exist in all chaotic systems, but according to the single-periodic-orbit theory (Bogomolny 1988, Berry 1989) the scar supporting region should shrink as $\sqrt{\hbar}$ as $\hbar \to 0$, whilst the probability density contrast remains fixed since it is predicted to be $\hbar$-independent (Heller 1984). The many-orbits theory (Robnik 1989) would speculatively predict the linear scaling of the scar area with $\hbar$ as a consequence of the interference effects. Some phenomenological material on this topic has been published recently in (Prosen and Robnik 1993a).

In this short section we would like to draw attention to an interesting scar-like feature seen in figure 3: near the boundary, about ten de Broglie wavelengths away, there is a thin scar-like feature, which has no simple explanation, because due to the non-convexity of the billiard boundary there are no Lazutkin-like caustics and invariant tori and also no such glancing periodic orbits. The only classical object that might be relevant for this feature is possibly the glancing orbit which survives many bounces while going round the boundary until reaching the non-convexity region and flying away, becoming completely chaotic afterwards. We have observed a few similar features in quite a

few other eigenfunctions, but we cannot offer any definite theoretical explanation so far. However, the formalism offfered and discussed in Müller *et al* (1993) might just be right to quantitatively describe the role of such orbits which are recurrent in configuration space but not periodic.

6. Discussion and conclusions

In this paper we have calculated numerically the high-lying chaotic states in the Robnik billiard as high as the 200 000th eigenstate and investigated their semiclassical morphology and their statistical properties. To achieve this we have implemented and adapted Heller's method of plane-wave decomposition, which has been further developed and its accuracy carefully checked. Similar to other workers (for example, Aurich and Steiner 1993) we reach the following conclusions. In such high-lying eigenstates the scars are hardly detectable since so far we have not found any of them. The average probability density is globally in excellent agreement with the theoretical semiclassical (and classical!) prediction. The Gaussian random model for the local statistical properties of the wavefunctions is generally excellent, in spite of the characteristic filamentary structure and the relevant clustering of probability density on the scale of a few tens of de Broglie wavelengths. This has been found by comparing the theoretical and the numerical distributions and also by the comparison of the lowest four moments and the evaluation of the Kolmogorov–Smirnov test. The autocorrelation function captures nicely the clustering property, and is found to be strongly direction-dependent in contradistinction with Berry's (1977b) isotropic prediction, but, after averaging over many directions, the agreement with Berry's theory is recovered. Finally we should mention that in some of the eigenstates we discovered scar-like features resembling the whispering-gallery modes, for which we do not have a proper theoretical explanation.

Our current and future work deals with the systematic search for the scars and the analysis of their geometry and scaling properties with $\hbar$. On the theoretical side the present paper stimulates further work on scar theory for which we expect improvement when a many-orbits theory has been set up, following the suggestions in Robnik (1989), Prosen and Robnik (1993a). Moreover, we believe that the application of Gutzwiller's (one-) periodic orbit theory could explain in detail the anisotropies of the autocorrelation function. Our work also shows that there is still much interesting structure over the range of a few tens of de Broglie wavelengths in chaotic wavefunctions, which calls for a more refined statistical description.

Acknowledgments

We wish to thank Boris V Chirikov for helpful comments and relevant references. The financial support by the Ministry of Science and Technology of the Republic of Slovenia is gratefully acknowledged.

References

Aurich R and Steiner F 1993 *Physica* **64D** 185
Berry M V 1977a *Phil. Trans. R. Soc.* **287** 237
——1977b *J. Phys. A: Math. Gen.* **10** 2083
——1983 Chaotic behaviour of deterministic systems *Proc. NATO ASI Les Houches Summer School* ed G Iooss, R H G Helleman and R Stora (Amsterdam: Elsevier) p 171
——1989 *Proc. R. Soc.* A **423** 219

Berry M V and Robnik M 1984 *J. Phys. A: Math. Gen.* **17** 2413
Bohigas O 1991 Chaos and quantum systems *Proc. NATO ASI Les Houches Summer School* ed M-J Giannoni, A Voros and J Zinn-Justin (Amsterdam: Elsevier) p 87
Bogomolny E B 1988 *Physica* **31D** 169
Bruus H and Stone A D 1994 *Dept. Phys. Yale University Preprint*
Casati G, Guarneri I and Smilansky U (eds) 1993 *Quantum Chaos* (Amsterdam: North-Holland)
Chirikov B V, Izrailev F M and Shepelyansky D L 1988 *Physica* **33D** 77
Frisk H 1990 Nordita *Preprint*
Giannoni M-J, Voros J and Zinn-Justin (eds) 1991 *Chaos and Quantum Systems* (Amsterdam: North-Holland)
Gutzwiller M C 1990 *Chaos in Classical and Quantum Mechanics* (New York: Springer)
Hayli A, Dumont T, Moulin-Ollagier J and Strelcyn J M 1987 *J. Phys. A: Math. Gen* **20** 3237
Heller E J 1984 *J. Phys. Rev. Lett.* **53** 1515
——1991 Chaos and quantum systems *Proc. NATO ASI Les Houches Summer School* ed M-J Giannoni, A Voros and J Zinn-Justin (Amsterdam: Elsevier) p 547
Heiler E J, O'Connor P W and Gehlen J 1987 *Phys. Rev. Lett.* **58** 1296
Markarian R 1993 *Nonlinearity* **6** 819
McDonald S W and Kaufman A N 1988 *Phys. Rev.* A **37** 3067
Müller K, Hönig A and Wintgen D 1993 *Phys. Rev.* A **47** 3593
Percival I C 1973 *J. Phys. B: At. Mol. Phys.* **6** L229
Press W H, Flannery B P, Teukolsky S A and Vetterling W T 1986 *Numerical Recipes* (Cambridge: Cambridge University Press)
Prosen T and Robnik M 1993a *J. Phys. A: Math. Gen.* **26** 5365
——1993b *J. Phys. A: Math. Gen.* **26** 2371
——1994a *J. Phys. A: Math. Gen.* submitted
——1994b *J. Phys. A: Math. Gen.* **27** L459
Robnik M 1983 *J. Phys. A: Math. Gen.* **16** 3971
——1984 *J. Phys. A: Math. Gen.* **17** 1049
——1989 *Preprint* Institute of Theoretical Physics, University of California Santa Barbara
——1994 *J. Phys. Soc. Japan Suppl.* **63**
Shapiro M and Goelman G 1984 *Phys. Rev. Lett.* **53** 1714
Shapiro M, Ronkin J and Brumer P 1988 *Chem. Phys. Lett.* **148** 177
Shnirelman A L 1979 *Usp. Mat. Nauk* **29** 181
Stone A D and Bruus H 1993 *Physica* **189B** 43
Stone A D and Bruus H 1994 *Surface Science* at press
Tél T and Ott E 1993 *Chaos Focus* (issue on chaotic scattering) **3**
Voros A 1979 *Lecture Notes in Physics 93* p 326